AD-A145 057 NRL (NAVAL RESEARCH LABORATORY) FEL (FREE ELECTRON LASER) PROGRAM(U) KM SCIENCES ARLINGTON VA 29 JUN 84 N00014-83-C-2041 1/1

UNCLASSIFIED F/G 20/5 NL

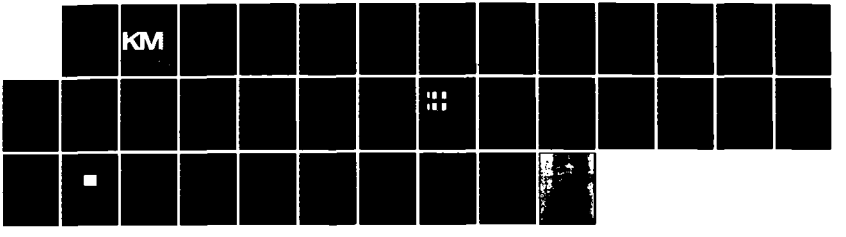

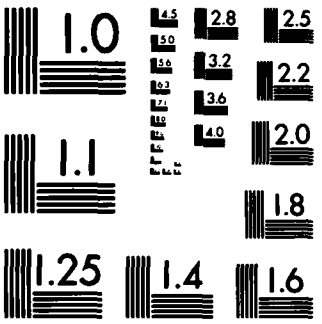

(12)

AD-A145 057

KMS SCIENCES
SCIENCES
SCIENCES
SCIENCES
SCIENCES
SCIENCES
SCIENCES

DTIC FILE COPY

DTIC
ELECTE
AUG 3 0 1984
H

84 08 02 044

FINAL REPORT IN SUPPORT OF THE NRL FEL PROGRAM

Work performed during the period 29, Dec., 82 to 29,June,84
This work is in fulfillment of the terms of
contract N00014-83-C-2042

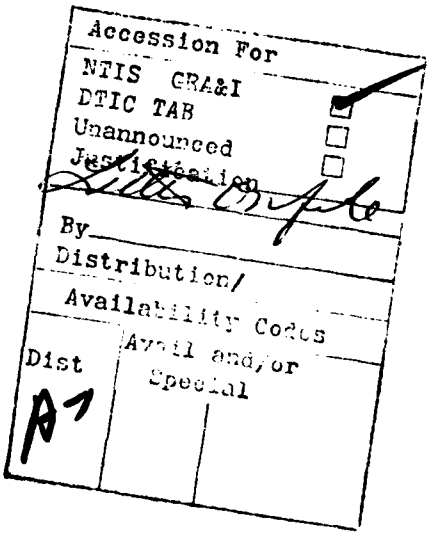

KM Sciences
1425 N. Nash St. #13
Arlington,VA 22209

INTRODUCTION

The Naval Research Laboratory, (NRL) Free Electron Laser, (FEL) program proposed to use the NRL Electron Linear Accelerator, (LINAC) as a source of relativistic electrons for its studies. Previous work by KM Sciences had concentrated on the evaluation of the upgrades needed on the entire facility to meet the needs of the FEL program. These had included injection electronics, injection hardware, accelerating structures, beam transport alignment, and the required additional deflection systems. The continuing work reported herein focuses on the design of a new injection system, beam quality evaluation, and on the design of an energy and phase analysis systems for the resultant electron beam. A computer ray-tracing program describing the interaction of the electron beam with the FEL wiggler structure will also be discussed.

DESIGN CONSIDERATIONS FOR IMPROVING THE INJECTION SYSTEM

INTRODUCTION

The NRL LINAC uses an iris loaded accelerating wave guide operated in the two pi over three mode to provide the accelerating field for the electron beam. The electrons which are accelerated remain bunched near the maximum of the r f field strength. This field is only purely longitudinal on the axis of the accelerating wave guide. Hence, if electrons are significantly off axis they will encounter some transverse momentum. For this reason it is advantageous to keep the electrons as near the axis as possible.

The present injection system for the NRL LINAC consists of an electron gun operating at 80 kv which produces a space charge limited beam of up to 20 Amperes. The minimum diameter of this beam is about one half inch at a point 3 to 4 inches from the output flange of the gun. A single lens about 10 inches from the gun refocuses the expanding beam to pass through an r f buncher and tapered beta preaccelerating section before entering the first section of accelerating wave guide. The appartures in the injection structures are the same as in the accelerating wave guide, about 1 inch. Since no means of limiting the diameter of the beam are provided, a considerable amount of the beam current is in a region of significant transverse field. This has two undesirable effects: first, a large part of the beam is lost; and second, some of the energy of the electrons in the transverse field regions excites higher modes of r f fields which further disturb what is left of the electron beam. This can cause a limiting effect on the maximum amount of beam one can put through the machine.

METHOD

The obvious approach to circumventing the above described difficulties is to limit the beam to as small a diameter as possible. However, one cannot increase the current density arbitrarily because the space charge forces will cause the beam to expand. One must therefore find a compromise between beam diameter and beam current.

A good treatment of space charge and electron beam production is found in chapter 7 of "Introduction to Electron and Ion Optics" by Poul Dahl, Academic Press, 1973. His treatment however, is nonrelativistic and since even at 80 kv an electron is traveling at about half the speed of light, this correction is significant. A relativistic treatment of Dahl's derivation is given in an appendix to this report. This results in the same differential equation (no. 26.2 in Dahl's text) with the relativistic correction changing the value of his constant, C. Dahl writes in his equation 26.3 that,

$$C=.00048xP,\ P=I/V^{3/2},$$

where I is the current in milliamperes, and V is the kinetic energy of the electron in kilo=electron volts. The relativistic form of this constant is,

$$C=1.17x10^{-7}I/(g^2-1)^{3/2},$$

where g is related to the electron kinetic energy by,

$$V=511(g-1),$$

I and V being in the same units as in the previous equation. Since C is a constant in the differential equation one can simply use the relativistically correct form in Dahls derived relations for beam waist , convergence, and emittance.

To estimate how small a diameter beam one can put through a LINAC one can proceed as follows:

Since one section of the LINAC about two meters long accelerates a fairly high current beam from about 2 MeV to 12 MeV we will use an average energy of 7 mev and will assume a useful current of 50 Amperes. It must be noted here that the electron bunch in the accelerator is only a few millimeters long, occuring every 10 centimeters. For an average current of 1 Ampere and a bunch length of 2 millimeters the bunched current will be 50 Amperes.This current and energy give a value of,

$$C=7.4x10^{-10}.$$

Dahl treats a case of the most nearly parallel beam which results in a waist diameter of .426 times the entrance diameter. For this case, the angle of convergence of the outermost electrons is given by,

$$A=(C/.585)^{1/2}.$$

Using the above value of C one gets A=.000036. For this case,the waist is at the middle of the accelerating section, 1 meter from an end with a diameter of .003 centimeters and an input diameter of .007 centimeters. These numbers clearly indicate that one can carry a considerable current in a very small beam. This result is only true because the electron was quite energetic. The real limitation is near the electron gun where the energy of the electron is only 80 KeV. At this region the buncher structure, which is 25 centimeters long, gathers electrons of 80 KeV of energy which are spread uniformly over 2 pi of r f phase and bunch them into about 60 degrees. This increases the current

density by a factor of 6. We will assume that we can use an average density 3 times as great as input over this region. Again one can calculate C and find,

C=.0018,

while the convergence angle becomes,

A=.055.

One finds that the waist diameter is .6 centimeters and the input diameter is 1.4 centimeters. Hence one can see that the injection region is the critical area in designing beam optics for the LINAC.

MODEL 12 GUN

Design data provided with the model 12 electron gun show that it will produce a current of about 20 Amperes through a waist diameter of about 1 centimeter at a point 9 centimeters from its output flange. These data indicate a value of C of .012 and a convergence angle of .143. It is reasonable to assume a uniform current density in the beam under such conditions. This would mean that an apparture .22 centimeters in diameter placed at the waist of the beam will pass a current of 1 Ampere.

SPACE LIMITATIONS

The LINAC is installed in room 105a of bld.75 with very little room to spare. There is only about 42 inches available for the entire injection system. The buncher section and the preaccelerator take up 30 inches of this, leaving only about 12 inches for lenses and a vacuum pump-out to the gun. Figure 1 is a schematic drawing of the system from the gun cathode to the input to the first section of accelerating wave guide. The system consists of an aperture followed by a lens to focus the beam through the buncher. Another lens is placed between the buncher and the preaccelerator. This is required to refocus the beam into the preaccelerator. The beam energy increases from 80 KeV to 2 MeV in this region hence no additional focusing is needed. An aperture is placed at the entrance to the first section of the LINAC to aid in adjusting the injection system. A lens is also placed between the gun and the first aperture. This will allow additional current to be focused through the aperture. This should prove useful in high current stored energy modes of operation.

LENS CALCULATIONS

As was shown earlier, there will be about 1 Ampere of beam at 80 KeV coming through a .22 centimeter diameter aperture with a divergence angle of 0.143. Because of the limited space, the lens will be 5.7 centimeters from the aperture. This means that the beam will expand to 1.6 centimeters at the center of the lens. This lens must refocus the beam to a waist at the middle of the buncher. This point is 18.2 centimeters from the center of the lens. The waist diameter at the center of the buncher will be 0.7 centimeters. The beam again expands back up to 1.6 centimeters at the center of the next lens. This lens must be set to produce a waist at about 12 centimeters in the preaccelerator. Since the beam will be gaining energy in this section it should exit with about a .6 or .7 centimeter

diameter. Using the thin lens formula,

$$1/f=1/p+1/q,$$

with an object distance of 5.7 centimeters and an image distance of 18.2 centimeters one calculates a focal length of 4.3 centimeters for the 2nd. lens (see fig. 1). The 3rd. lens operating with an 18.2 centimeters object distance and an image distance of about 12 centimeters will have about a 7 centimeter focal length.

There is only limited space for a lens between the gun and the first aperture. This lens is designed to be as strong as one can put into this limited space.

MAGNETIC LENS DESIGN

The lenses are magnetic coils with soft iron pole faces designed using tables and formulae from "Electron Beams, Lens, and Optics", Vol. 1, by Kareh and Kareh, Academic Press,1970. The previously determined beam diameter and lens focal length provides a starting point from which to proceed in designing a suitable lens.

It was found that the beam expanded to 1.6 centimeters in diameter at the center of the lens hence this lens must have an inside diameter which is at least as great if it is not to restrict the beam. A basic parameter of lens design is the ratio of gap width,S, to bore diameter,D. A reasonable choice for the space available S/D=0.4. If this parameter is made too small the ratio of field strength at the pole tips to the field strength on the axis of the lens becomes too great and one has difficulties with saturation of the iron.

Table 8.2b of Kareh and Kareh indicate that about 1500 Ampere turns will be needed to achieve a focal length of 5 centimeters for a lens of 1.6 centimeter bore. This can be easily achieved in the space available with 150 turns of #10 copper wire. However, there is a further consideration, and that is the fact that this coil will produce a field of 1.5 Tesla in the iron and iron begins to saturate around 1 Tesla. To ensure that a sufficient field strength is achieved at the gap the pole tips must be tapered back about 55 degrees according to Kareh's text.

MEASUREMENT OF THE EMITTANCE OF THE NRL LINAC BEAM

INTRODUCTION

KM Sciences undertook as its part in a program of FEL research at NRL, to upgrade the performance of the NRL LINAC. The FEL experiment was designed around a 30 MeV electron beam from the NRL LINAC. For the experiment to be successful this beam must have about a 1% energy spread, a pulse length of 1 microsecond, a macro-pulse current of 100 milliamperes, and an emittance of less than 3 Pi millimeter-milliradians.

In order that the NRL LINAC meet these rather stringent requirements on its beam quality, a great many improvements were required. The upgrade on the injection system was previously described. The emittance of the electron beam is a significant measure of the performance of the upgraded injection system.

METHOD

The emittance of a beam of charged particles is represented by the area in phase space, of that beam at a given beam energy. If there are no interactions involving an energy exchange with the outside world, the emittance of the beam is a constant, independent of such things as focusing or deflection. The emittance of a cylindrically symmetrical beam may be expressed as:

$$e=\pi x'x \ ,$$

where x' is the angle of a particle's trajectory and x is the position of the particle with respect to the beam axis. If one plots these two quantities, x' and x, for each particle in the beam one would find that they fall within an ellipse. The area of this ellipse is the emittance of the beam.

One method of experimentally determining the emittance of a beam is known as " the pepper pot". This is shown schematically in figure 2. A glance suffices to show that the divergence is:

$$x'_i=(h_i-x_i)/S.$$

If one measures a number of these angles and positions, one can generally find a circumscribed ellips which just contains all of the points so defined. One must ensure that the holes in the pepper pot diaphragm extend beyond the beam spot incident upon it in order to measure the entire beam. For the NRL experiment, the diaphragm consisted of a brass plate with a crossed array of holes .031 inches in diameter spaced .060 inches on centers and extending either side of the center by .450 inches. The diaphragm is shown in figure 3. This diaphragm was mounted inside the vacuum plumbing on an energy analyzed beam line from the NRL LINAC. The electrons which passed through the holes were detected on a P15 phosphor screen deposited on a glass plate which also formed the vacuum barrier. This plate had a .600 inch diameter circle engraved on its inner surface to provide a dimensional calibration. The screen was approximately 1 meter from the pepper pot diaphragm. The screen was viewed through a closed circuit television system. A close-up lens configuration provided sufficient magnification for the image of the calibration circle to nearly fill the tv screen. A video cassette recorder was used to record the images of the holes in the diaphragm and of the calibration circle. This technique allowed the playback with "stop action" which provided a stationary image on the monitor. This greatly facilitated measuring the positions and sizes of the images of the pepper pot holes that were produced by the LINAC electrons.

THE MEASUREMENTS

The LINAC was tuned at 33 MeV, the exact energy not being critical to this experiment. A pulse current of about 200 milliamperes was achieved through an energy selecting slit system which was set to pass a 2% energy band. The pulse width was greater than 1 microsecond. The beam was steered to be centered on the pepper pot diaphragm and the screen was adjusted such that

the image of the holes in the pepper pot were centered on the screen. The tv camera was stopped down to f/4 to improve the image sharpness. The LINAC was single pulsed with the dot pattern appearing on each pulse. A number of dot patterns were recorded with very little variation from one to another.

The beam was not cylindrically symmetric; hence, both a horizontal and vertical emittance was measured. Figure 4 is a plot of the measured points for each case together with the circumscribed ellipse. The areas of these ellipses gave the horizontal and vertical emittances. The vertical emittance was found to be 1.35+or-.2 Pi millimetre milliradians, and the horizontal emittance was found to be 1.7+or-.2 Pi millimeter milliradians. These results indicate that the LINAC was producing a beam of suitable quality for the FEL experiment.

ENERGY ANALYZER

A magnetic spectrometer magnet was set up as a dump magnet for the electron beam after it exited the FEL experiment. This magnet was deiscribed in a previous report. The positions of the electron arriving at the focal plane of this magnet are detected by the Cherenkov radiation they produce in ultra pure quartz optical fibers. These fibers are arranged like teeth of a comb along the focal plane. The spacing for the dispersion of the magnet gave an energy resolution of 0.2%. The other ends of the fibers were bundled into a rectangular array and optically coupled to the face of the vidicon of an RCA TC1005 camera in such a fashion that the scan of the beam of the vidicon traveled from one end of the comb to the other. Thus the composit video signal from the camera would display the positions of the electrons as they arrived at the focal plane of the magnet, scanning from high energy to low. That is, the energy of the electrons would be shown as a time distribution during the composit video signal.

A proof of principle experiment was performed using the electron beam from the NRL LINAC. A small linear array of fibers was placed such that the electron beam exiting a window in the LINAC beam plumbing would strike part of the linear array. The other ends of the fibers were placed on the window of the vidicon. The composit video signal was connected to an oscilloscope. By adjusting the orientation of the fibers at the vidicon one could line them up with the scanning trace of the vidicon and clearly "see" where the LINAC beam was hitting the linear array of fibers.

Initial designs for the associated hardware for this energy measuring system were presented to NRL for design and drafting and construction. The termination of the program by NRL prevented any further work on this system.

MICRO-BUNCH ANALYSIS

Electrons accelerated in the NRL LINAC receive their energy from a traveling r f wave at a frequency of 2858 megaHertz. Since the electrons only "see" an accelerating field over a relatively small part of the r f cycle, they are bunched into micro pulses about 35 picoseconds long and separated from each other by 350 picoseconds. It is useful both in tuning the LINAC, and in understanding the behavior of the FEL, to have a measure of the actual length of these microbunches.

METHOD

Such a train of pulses of charge will generate an electromagnetic spectrum which may be detected and analyzed to yield information on bunch length and separation. If one assumes that the pulses have a cosine squared shape with a spacing of T, equal to 350 picoseconds and a base line width of t_o of about 35 picoseconds then the coefficients of the spectral componants will be given by;

$$C_n = 2A\{\sin(b)/bX[1-(b/Pi)^2]\}.$$

This means that the first harmonic will appear at a frequency of T/t_o times the fundamental at 2858 megaHertz. The more tightly the electrons are bunched, the smaller will be t_o and consequently the higher will be the frequency of the first harmonic. KM Sciences recommended that a small pickup loop be placed in the LINAC beam line which would be of a low enough inductance to detect about 100 megaHertz. This signal would then be analyzed by a Tektronics spectrum analyzer. Because the FEL program at NRL was terminated, NRL did not act on this recommendation.

ELECTRON TRAJECTORIES THROUGH A LINEAR WIGGLER CALCULATED WITH A THREE DIMENSIONAL RAY TRACING PROGRAM

Considerable theoretical work has been done on the calculation of electron trajectories through free electron laser wiggler structures. Most of these, however, have treated the magnetic field in a somewhat simplified manner describing a field only on axis and far from any end effects. In this paper we will describe a method of calculating the trajectories of electrons through a finite length linear wiggler structure including fringing effects.

BASIC RAY TRACING EQUATIONS

The well known Lorentz force acting on a charged particle moving in a purely magnetic field is:

$$F=VxBe/c. \tag{1}$$

Since the force is always perpendicular to the velocity, the relativistic form of Newton's force law can be written as:

$$F=gm_od(V)/dt. \tag{2}$$

(Here the letter g is used for the relativistic energy in mc^2 units instead of the more familiar symbol, gamma.) Combining equations 1 and 2 gives the following set of relations:

$$dv_x/dt=(v_yb_z-v_zb_y)e/gm_oc, \tag{3a}$$

$$dv_y/dt=(v_zb_x-v_xb_z)e/gm_oc, \tag{3b}$$

$$dv_z/dt=(v_xb_y-v_yb_x)e/gm_oc. \tag{3c}$$

Figure 5 shows the coordinate system used to make the ray-tracing calculations. If one knows the velocity and position of a partical at a given instant and can calculate the value of the magnetic field at that point, one can determine each component of change in velocity during a short time interval. Since the velocity of the particle in the wiggler is mostly in the z direction, one chooses small steps in that direction and calculates the time required for the step. The program used for the ray-tracing calculations, the velocity before the step plus half the change in velocity during the step as the average velocity during the step. This velocity is then used to calculate the new position of the particle after the time interval, dt. Thus one arrives at a new set of positions and velocities where one again calculates the magnetic field and repeats the entire

This method was first tried using an analytic expression for the magnetic field. A suitable form for a linear wiggler is:

$$B_y=-B_o\cosh(k_w y)\sin(k_w z), \tag{4a}$$

$$B_z=-B_o\sinh(k_w y)\cos(k_w z). \tag{4b}$$

Ray tracing calculation using the above expressions for the magnetic field were carried out through a 60 period wiggler and gave the expected trajectories. They showed an oscillating path about a straight line in the x,z plane and a slow betatron oscillation in the y,z plane. These results indicated that the program was working correctly. The field described by equations 4 does not provide for any fringing fields at the beginning and end of the wiggler. What was needed was a more realistic description of a wiggler field.

A MORE REALISTIC MAGNETIC FIELD

The NRL Free Electron Laser Experiment will use a "Halbach" configuration of rare-earth-cobalt magnets to produce its wiggler field. This configuration has already been shown in figure 5. Each period of the wiggler consists of 4 pairs of magnets. These pairs of magnets are of two distinct types which will be labeled A and B. Since there is no material with a differential permeability other than unity throughout the wiggler, the magnetic field at any given point is simply the vector sum of the contributions from all the magnets close enough to make a significant contribution.

It was assumed that the magnets consisted of a uniform distribution of infinitely small dipoles of density m per unit volume. It was further assumed that the magnets extended infinitely far in the x direction. This will result in there being no x component to the magnetic field.

Figure 6 shows the dimensions used to derive the field relations for an A Type magnet. The relations for the magnetic field far from a point dipole are:

$$dB_r=2mdv\cos(g)/r^3, \tag{5a}$$

$$dBb_\theta=mdv\sin(g)/r^3, \tag{5b}$$

and from the geometery of figure 6 one can write;

$$dB_{ry}=2mdv\cos^2(g)/r^3 \tag{6a}$$

$$dB_{rz}=2mdv\cos(g)\sin(g)\cos(h)/r^3 \tag{6b}$$

$$dB_{rx}=2mdv\cos(g)\sin(g)\sin(h)/r^3 , \tag{6c}$$

for the components of the radial term, and;

$$dB_{gy}=-mdv\sin^2(g)/r^3 \quad (6d)$$

$$dB_{gz}=mdv\sin(g)\cos(g)\cos(h)/r^3 \quad (6e)$$

$$dB_{gx}=mdv\sin(g0\cos(g)\sin(h)/r^3; \quad (6f)$$

for the components of the angular term. Figure 7 shows the geometry for integrating over x . From this figure one can arrive at the following substitution relations:

$$r^2=(X-x)^2+y^2+z^2 \quad (7a)$$

$$\cos(g)=y/r \quad (7b)$$

$$\sin(g)=[(X-x)^2+z^2]^{1/2}/r \quad (7c)$$

$$\cos(h)=z/[(X-x)^2+z^2]^{1/2} \quad (7d)$$

$$\sin(h)=(X-x)/[(X-x)^2+z^2]^{1/2}. \quad (7e)$$

By combining equations 6 and 7 one gets:

$$dB_{ry}+dB_{gy}=mdv\{2y^2/r^5-[(X-x)^2+z^2]/r^5\} \quad (8a)$$

$$dB_{rz}+dB_{gz}=mdv\{2yz/r^5+yz/r^5\} \quad (8b)$$

$$dB_{rx}+dB_{gx}=mdv\{2y(X-x)/r^5+y(X-x)/r^5\}. \quad (8c)$$

Figure 8 shows the geometry for a "B" type magnet. For this geometry and the same relations for the dipole fields one can write the following set of differential equations:

$$dB_{rz}=2mdv\cos^2(g)/r^3 \quad (9a)$$

$$dB_{rx}=2mdv\cos(g)\sin(g)\cos(h)/r^3 \quad (9b)$$

$$dB_{ry}=2mdv\cos(g)\sin(g)\sin(h)/r^3 \quad (9c)$$

$$dB_{gz}=-mdv\sin^2(g)/r^3 \quad (9d)$$

$$dB_{gx}=mdv\sin(g)\cos(g)\cos(h)/r^3 \quad (9e)$$

$$dB_{gy}=mdv\sin(g)\cos(g)\sin(h)/r^3. \quad (9f)$$

The replacement relations for the "b" geometry are:

$$r^2=(X-x)^2+y^2+z^2 \quad (10a)$$

$$\cos(g)=z/r \quad (10b)$$

$$\sin(g)=[(X-x)^2+y^2]^{1/2}/r \quad (10c)$$

$$\cos(h)=(X-x)/[(X-x)^2+y^2]^{1/2} \quad (10d)$$

$$\sin(h)=y/[(X-x)^2+y^2]^{1/2}. \quad (10e)$$

By combining equations 9 and 10 one gets the following set of differential equations for the "B" type magnets:

$$dB_{r_z}+dB_{\theta_z}=mdv\{2z^2/r^5-[(X-x)^2+y^2]/r^5\} \quad (11a)$$

$$dB_{r_x}+dB_{\theta_x}=mdv\{2z(X-x)/r^5+z(X-x)/r^5\} \quad (11b)$$

$$dB_{r_y}+dB_{\theta_y}=mdv\{2zy/r^5+zy/r^5\}. \quad (11c)$$

One now integrates with respect to x from minus infinity to plus infinity and one gets for a line of dipoles of the "A" type:

$$dB_y=2mda(y^2-z^2)/(y^2+z^2)^2 \quad (12a)$$

$$dB_z=4mdayz/(y^2+z^2)^2, \quad (12b)$$

and for a line of dipoles of the "B" type:

$$dB_z=2mda(z^2-y^2)/(y^2+z^2)^2 \quad (13a)$$

$$dB_y=4mdayz/(y^2+z^2)^2. \quad (13b)$$

Note that the x components have vanished as one would expect, and that one now has a differential of area, da. Figure 9 shows the geometry used to integrate over finite dimensions in the z and y directions. For an "A" type one then can write:

$$dB_y=2mda[(Y-y)^2-(Z-z)^2]/r^4 \quad (14a)$$

$$dB_z=4mda(Y-y)(Z-z)/r^4, \quad (14b)$$

and for the "B" type:

$$dB_z=2mda[(Z-z)^2-(Y-y)^2]/r^4 \quad (15a)$$

$$dB_y=4m(Y-y)(Z-z)/r^4. \quad (15b)$$

From figure 9 one can see that the limits of integration with respect to z are from z-b/2 to z+b/2 and with respect to y from y-c/2 to y+c/2. Designating the z limits as z_1 and z_u respectively and the y limits as y_1 and y_u respectively one gets, after carrying out the integration for the "A" type magnet:

$$B_y=2m(\tan^{-1}(z_1/y_1)-\tan^{-1}(z_u/y_1)-\tan^{-1}(z_1/y_u)+\tan^{-1}(z_u/y_u)) \quad (16a)$$

$$B_z=-m[\ln(y_1^2+z_1^2)-\ln(y_1^2+z_u^2)-\ln(y_u^2+z_1^2)+\ln(y_u^2+z_u^2)] \quad (16b)$$

and for the "B" type magnets:

$$B_z=-2m(\tan^{-1}(z_1/y_1)-\tan^{-1}(z_u/y_1)-\tan^{-1}(z_1/y_u)+\tan^{-1}(z_u/y_u)) \quad (17a)$$

$$b_y=-m[\ln(y_1^2+z_1^2)-\ln(y_1^2+z_u^2)-\ln(y_u^2+z_1^2)+\ln(y_u^2+z_u^2)]. \quad (17b)$$

In order to have the field due to a pair of magnets one can displace the center of a magnet up a distance a, and the center of a second magnet down a distance a. One must then replace y by y-a for the upper magnet and y by y+a for the lower magnet. Also, for the "B" type magnets the lower magnet is reversed so that the overall sign of the bottom magnet in the "B" type must be negative.

These equations allow one to calculate the magnetic field due to either an A pair or a B pair of magnets assuming that the magnets are infinitely long in the x direction. Figure 10 shows a plot of the y component of the field on axis calculated with the above derived relations. Figure 11 is included for completeness to show that the z component of the fields are zero on axis. Figure 12 shows the z component of the field 5 millimeters off axis. This clearly shows the effect sharp corners of the magnets introducing higher spatial frequency terms into the fields.

It is also apparent from the previous figures, that the fields extend well beyond the edges of the individual magnet pairs. A program was written to sum the effects of many magnet pairs to evaluate the field at a given point. It was found that summing over two periods of the wiggler is sufficient to provide an accurate field value at the center of this structure. Figure 13 is the y component of the field on axis for a two period structure. The z component on axis is zero as before, and figure 14 shows the z component 5 millimeters off axis. Again the higher spatial frequency terms are quite apparent.

In order to calculate the field in an N period wiggler, the following procedure was devised. First the field was calculated by summing over the first two periods of the wiggler to obtain the strength starting at a point two periods outside of the wiggler and continuing into the wiggler one period. At this point the scheme was changed to sum from one period behind the point of consideration to one period in front. This was continued through the wiggler adding a new magnet pair at the front and dropping a magnet pair at the back as each new magnet pair was encountered. At one period inside the end of the wiggler this procedure was stopped and the contributions of the last two periods were used to calculate the fields to a point two periods outside the wiggler. Figure 15 shows the results of such a calculation for a 30 period wiggler. The plot is the y component on axis. With this method it was relatively easy to include the effects of an additional magnet pair placed at the entrance end of the wiggler to compensate for the direction of the electron. The plot in figure 15 includes such a magnet pair.

THE FINITE X DIMENSION

The discussion to this point provides a method to calculate the magnetic field for a finite length wiggler constructed with magnet pairs whose x dimension is infinitely long. This results in no x component to the magnetic field and is useful to observe some of the physics of an electron passing through such a structure. However it is of interest to include effects of the finite length of the magnet pairs since in many experiments the ratio of gap to length of these magnet pairs

greater than .2. Measurements of the y component as a function of x for the geometry used at NRL, (a gap of 1.5 cm and a length of 5 cm), indicated an x^4 dependence with a 2% decrease per cm away from the axis. Such a dependence was included in the ray tracing program without difficulty. The coefficient of the x^2 term was an adjustable parameter allowing its effect to be turned on and off from run to run so that the effect on the trajectory could be seen.

This correction is still not complete since the x component of the field is zero. Although the x component is zero both in the x=0 and the y=0 planes of a real wiggler structure it does not remain 0 as one departs from the x=0 plane either above or below the y=0 plane. The following form for the x component of the magnetic field was chosen as providing all of the required properties;

$$b_x=(-ka/l)(x-x^5)\sinh(k_w y)\cos(k_w z). \qquad (18)$$

Here a is the same spacing of the magnets above and below the mid plane as was used in the previous derivation, and l is the length of the magnets in the x direction. The value of k of .02 gave a fairly close agreement with measurements made for the NRL structure.

As before, the coefficient, k, and the magnet length, l, were adjustable parameters in the ray tracing program, allowing the effect of the x componant of the wiggler field to be turned on as desired.

Figure 16 is an example of the output of the complete raytracing code for the parameters of the NRL FEL wiggler. It shows the trajectory of the electron in the horizontal and the vertical planes. The horizontal plane exhibits the sinesoidal path expected due to the periodic nature of the magnetic field. The compensating magnet has been adjusted to allow the trajectory to very nearly parallel the axis of the FEL wiggler structure. The vertical plane shows the long period betatron oscillation characteristic of such structures when the electron enters off axis.

THE RAY TRACING CODE

The program developed by KM Sciences is a menue driven code allowing adjustable parameters for the electron beam and for the wiggler structure. The electron beam parameters are; energy, initial x position and direction, and initial y position and direction. The wiggler parameters are; the maximum magnetic field strength on axis, the coefficient of the x dependence, the length of the magnets, the width of the magnets, the separation of the magnets from each other, the spacing above and below the wiggler axis, the position with respect to the entrance of the wiggler of a compensating magnet, the spacing of the compensating magnet above and below the axis, and the strength of the compensating magnet.

Appendix 1

Relativistic Space-Charge Limited Electron Beams

Consider a cylindrical beam of electrons all moving with a velocity, v, only in the positive z direction. The force acting on an electron in the beam is given by the relativistically invariant Lorentz force equation,

$$F=e(E$$

Appendix 1

Relativistic Space-Charge Limited Electron Beams

Consider a cylindrical beam of electrons all moving with a velocity, v, only in the positive z direction. The force acting on an electron in the beam is given by the relativistically invariant Lorentz force equation,

$$F=e(E+V\times B), \tag{1}$$

which, in the above situation, reduces to only a radial term. In cylindrical coordinates this is,

$$F(\text{radial})=e[E(\text{radial})-V\times B(\text{angle})]. \tag{2}$$

From Gauss's law one finds that the electric field is only due to electrons closer to the axis than the one under consideration. In MKS units the electric field is,

$$E(\text{radial})=q/2\times PI\times R\times A, \tag{3}$$

and

$$A=10^{7}/4\times PI\times C^{2},$$

where R is the radius of the beam, and q is the charge inside a unit length of the beam. This charge can be represented in terms of the current as,

$$q=I/V. \tag{4}$$

By using equation (4) in (3) and inserting the value of A one gets,

$$E(\text{radial})=2\times 10^{-7}\times I\times C^{2}/R\times V. \tag{5}$$

Ampere's law gives the magnetic field for a current wholly within the path of integration. This field expressed in MKS units is then,

$$B(\text{angle})=u\times I/2\times PI\times R, \tag{6}$$

where $u=4\times 10^{-7}\times PI$. Expressions (5) and (6) can be put in (2) to give,

$$F(\text{radial})=2\times 10^{-7}\times e\times I[(C^{2}/V)-V]/R. \tag{7}$$

Conventional notation in special relativity writes V/C as beta, and the quantity, square root of 1-beta squared as 1/gamma.(in this report we will write gamma as G.) Using this symbol one can write equation (7) as,

$$F(\text{radial})=2\times 10^{-7}\times e\times I\times C^{2}/R\times V\times G^{2}. \tag{8}$$

The relativistic form of Newton's law is,

$$F=G\times m\times a. \tag{9}$$

where m is the rest mass and a is the acceleration. If we assume that the velocity of the electron in the radial and angular directions is much smaller than in the z direction we can write,

$$a=V^2\times R'', \tag{10}$$

where the notation R" stands for the 2nd darivative of R with respect to z. Using (9) and (10) in (8) we can write,

$$R''=K/R, \tag{11}$$

where,

$$K=2\times 10^{-7}\times e\times I\times C^2/m\times(V\times G)^3. \tag{12}$$

This is the same as equation 26.2 in Poul Dahl's text with a different value of the constant. The velocity can be eliminated from (12) to give,

$$F(radial)=(2\times 10^{-7}\times e/m\times C)\times I/(G^2-1)^{1.5}. \tag{13}$$

The quantity G can be found from,

$$T=(G^2-1)m\times C^2, \tag{14}$$

with T being the kinetic energy of the electron. The constant, K, can be written in a form which allows a comparison with Dahl's constant,

$$K=1.17\times 10^{-7}\times I/(G^2-1)^{1.5}, \tag{15}$$

where T of equation (14) is in KeV, and the current, I, is in milliamperes. At 80 KeV the electron's velocity is about half of the velocity of light. If one assumes 1 ampere of 80 KeV electrons, using equation (15) one gets,

$$K=.000596,$$

while Dahl's equation 26.3 gives,

$$K=.000670.$$

The correction is already about 12% and becomes larger with increasing energy.

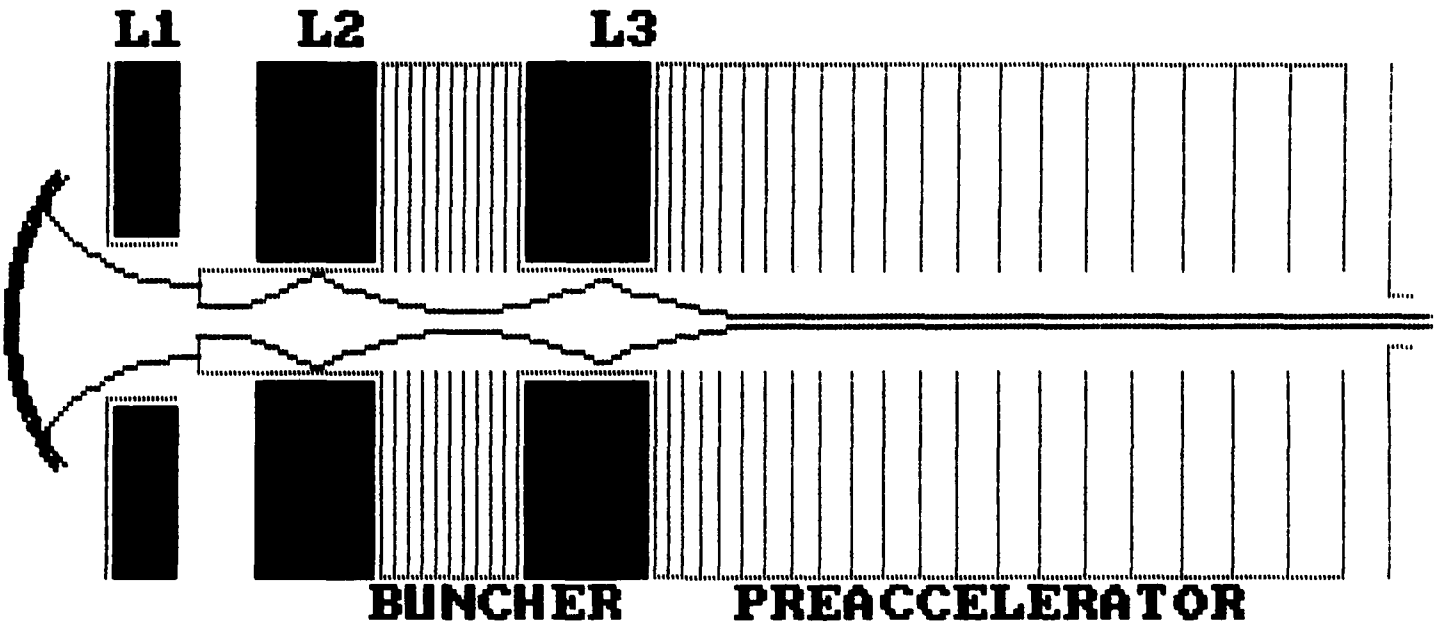

Figure 1. A schematic drawing of the redisigned injection system for the NRL LINAC.

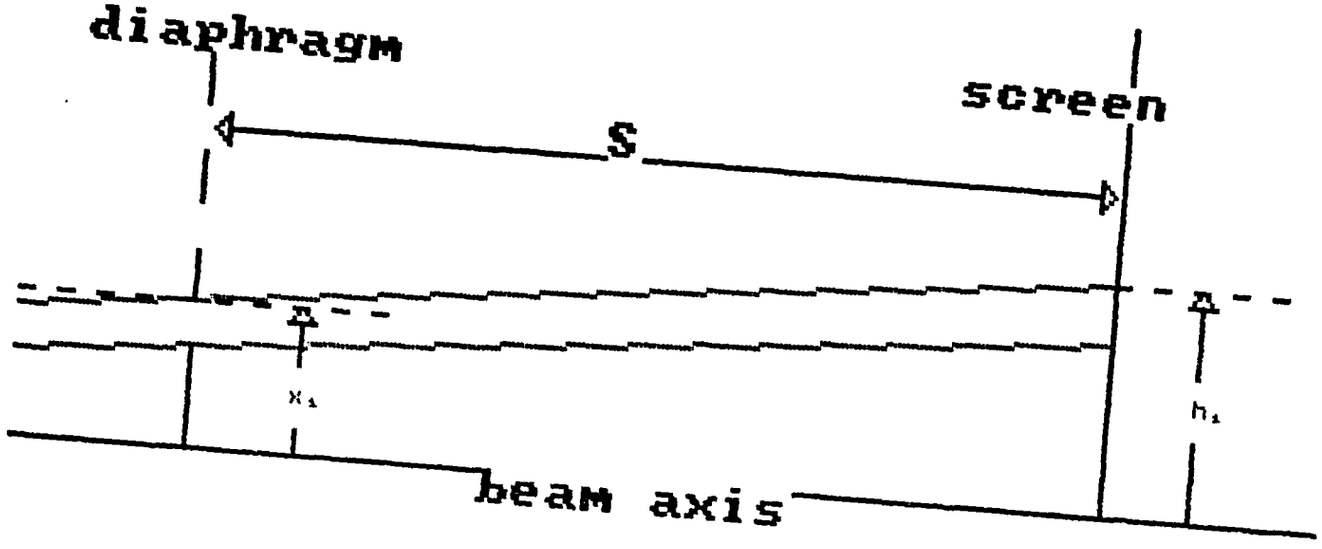

Figure 2. The points x_i, are the distances from the beam axis at the diaphragm, and the points h_i, the corresponding locations of electron arrival at the screen.

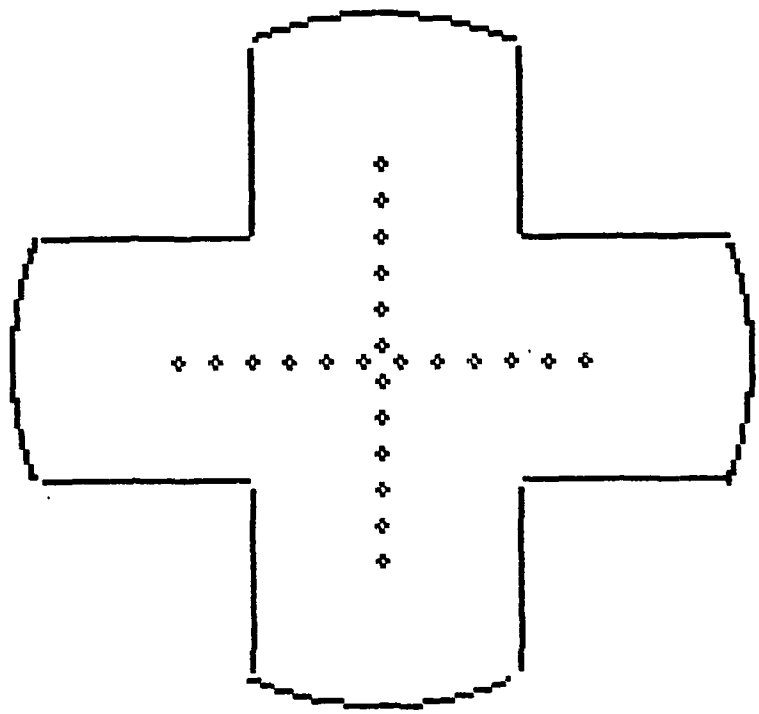

Figure 3. The diaphragm used in the NRL emittance measurement.

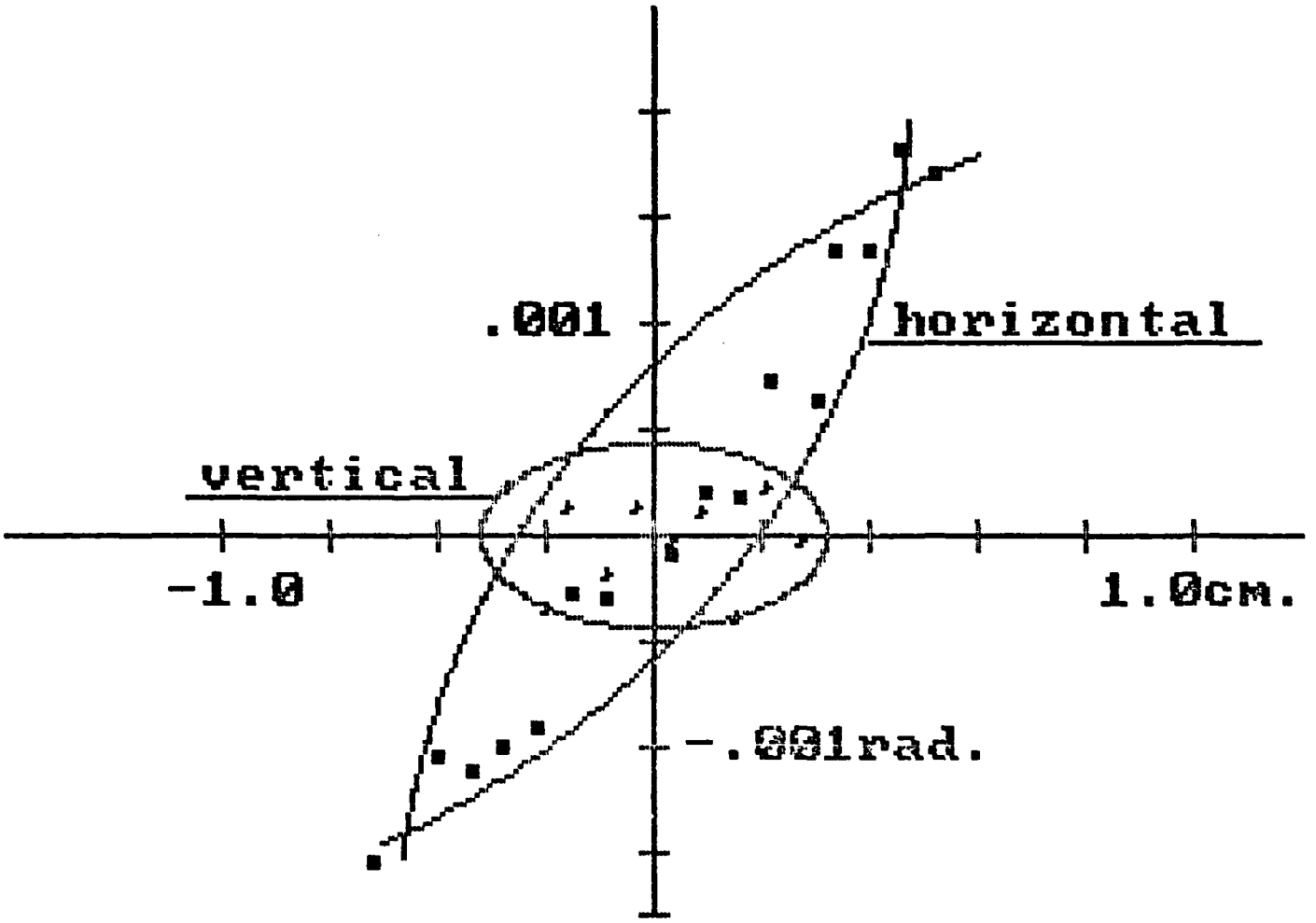

Figure 4. The emittanc ellipses for the NRL beam. The vertical axis is in 1/2 milliradians,and the horizontal axis in 1/4 centimeters.

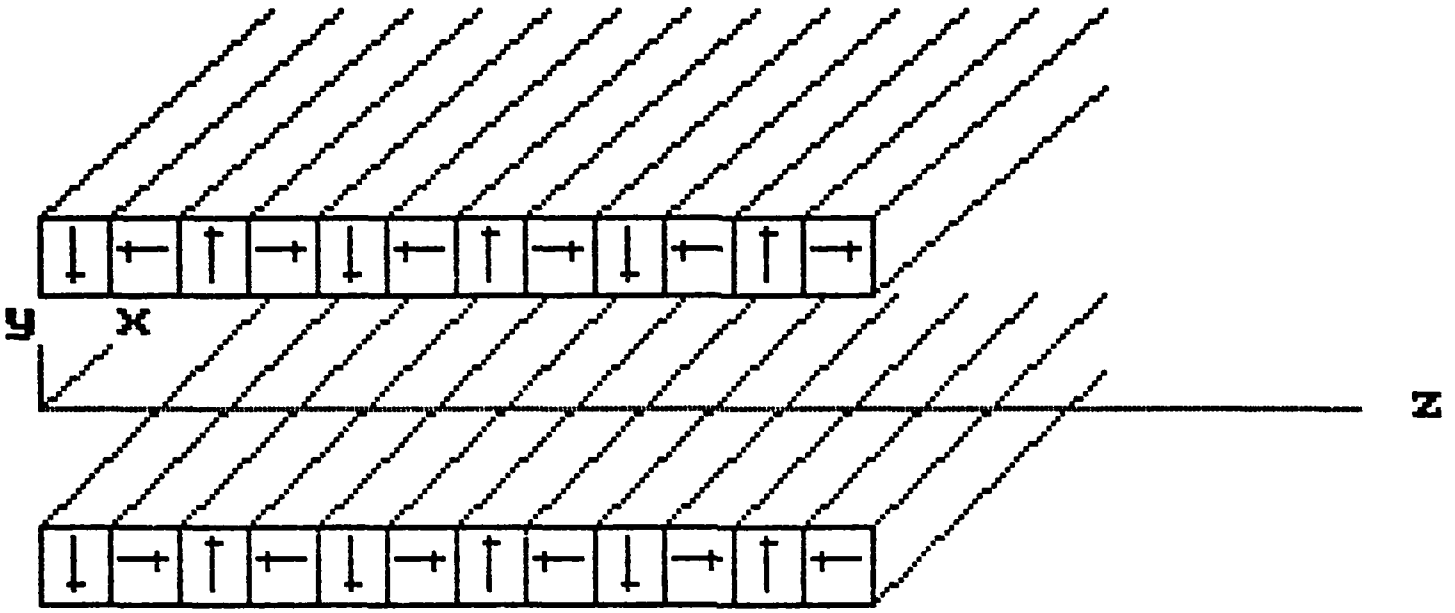

Figure 5. The geometry of the NRL FEL wiggler indicating the "Halbach" configuration.

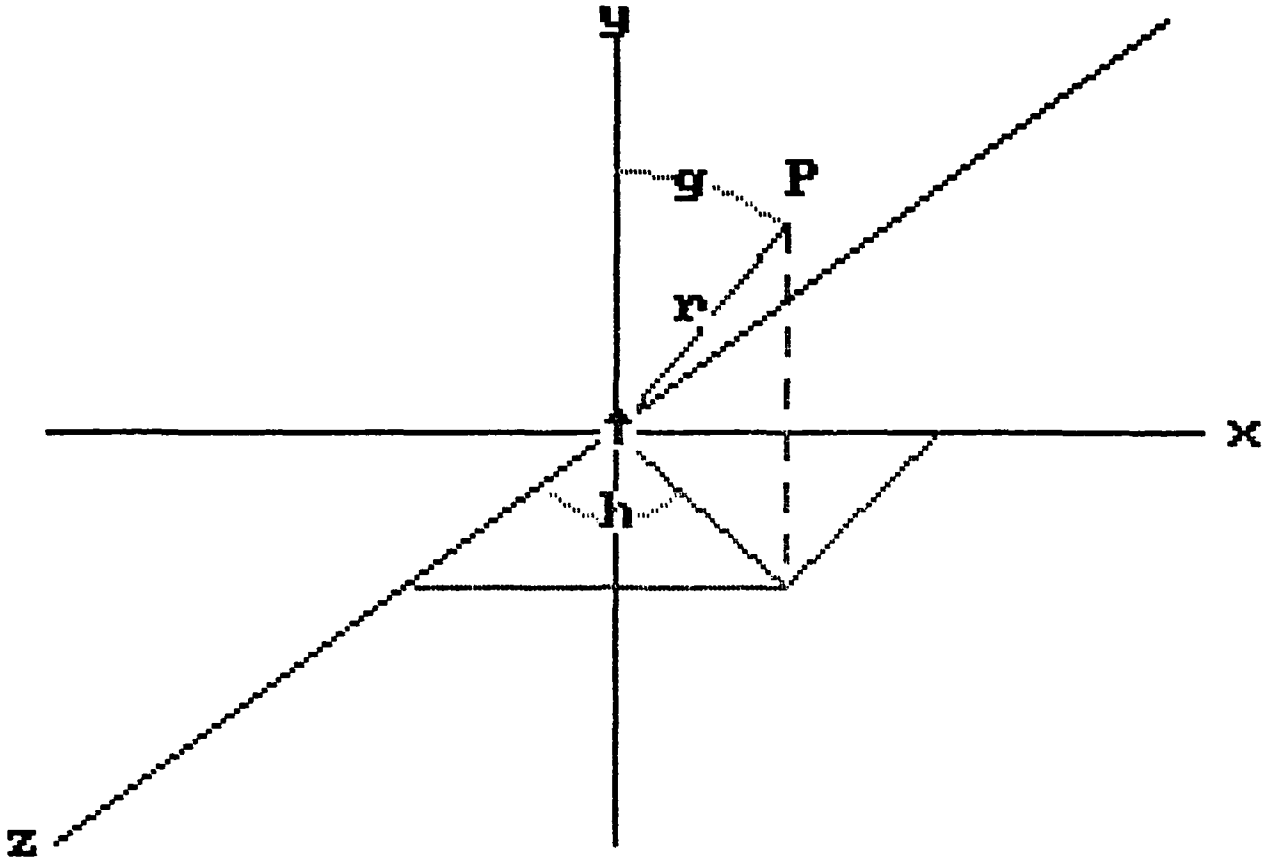

Figure 6. The coordinate system for deriving the field components for the "A" magnet configuration.

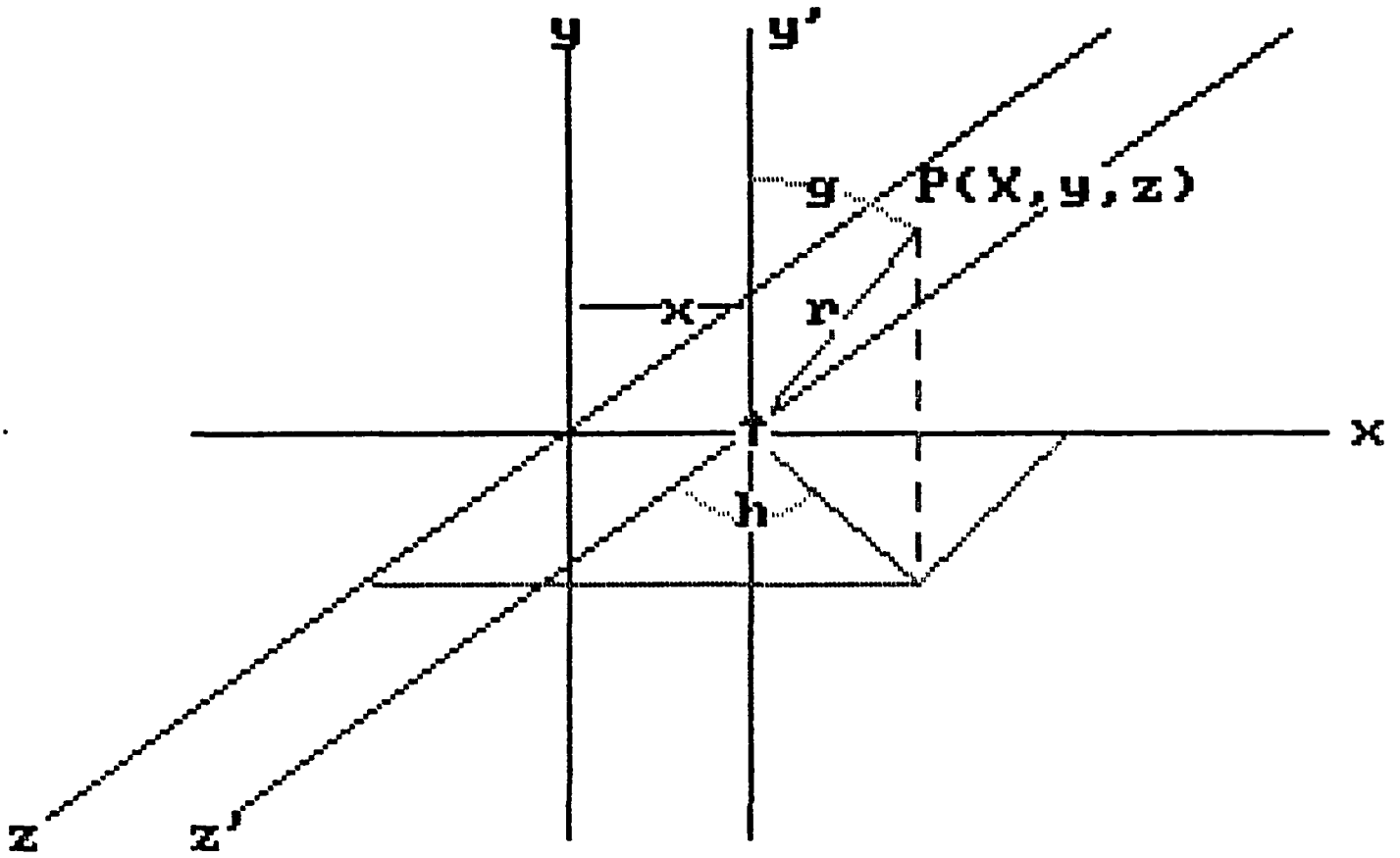

Figure 7. This shows the transformation used to integrate over the x coordinate.

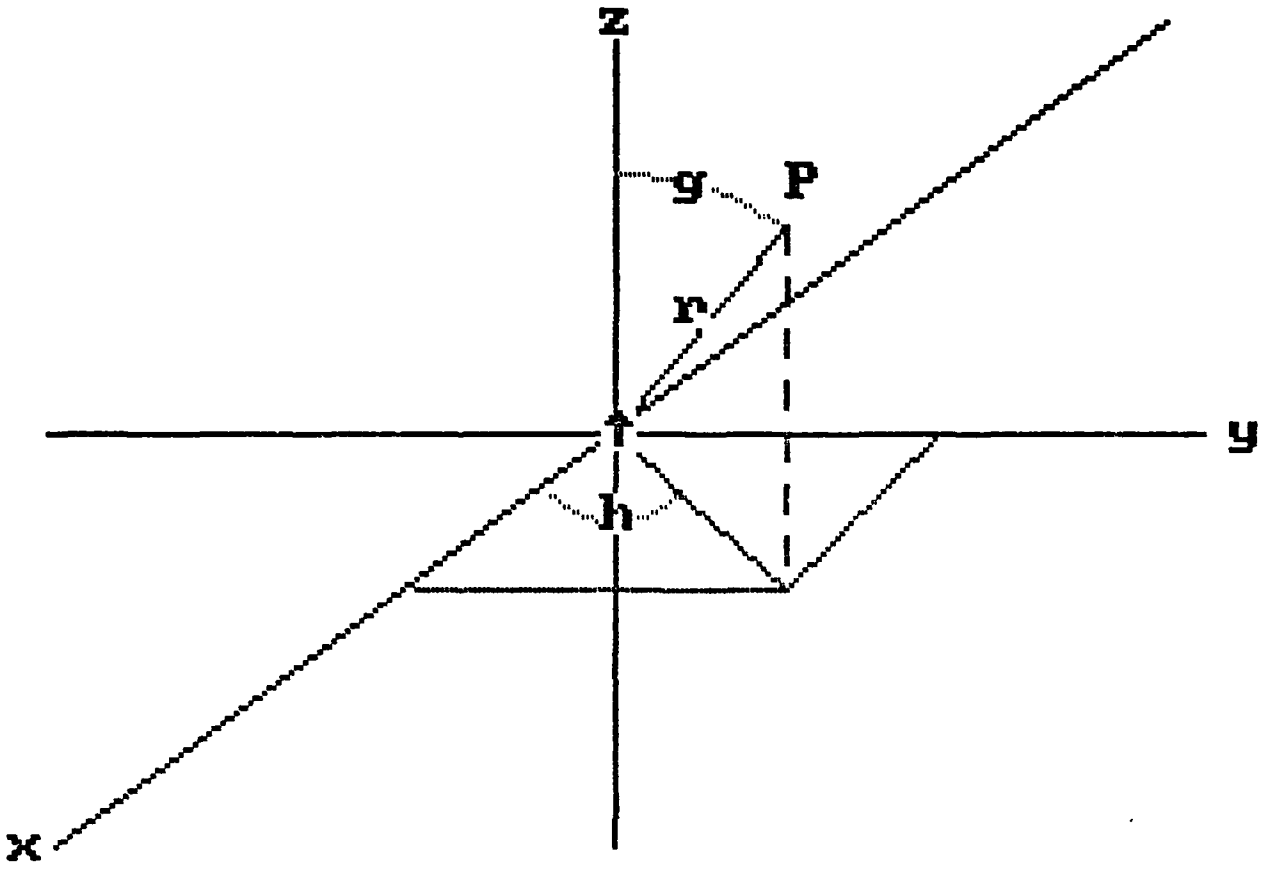

Figure 8. The coordinate system used for deriving the field components for the "B" magnet configuration.

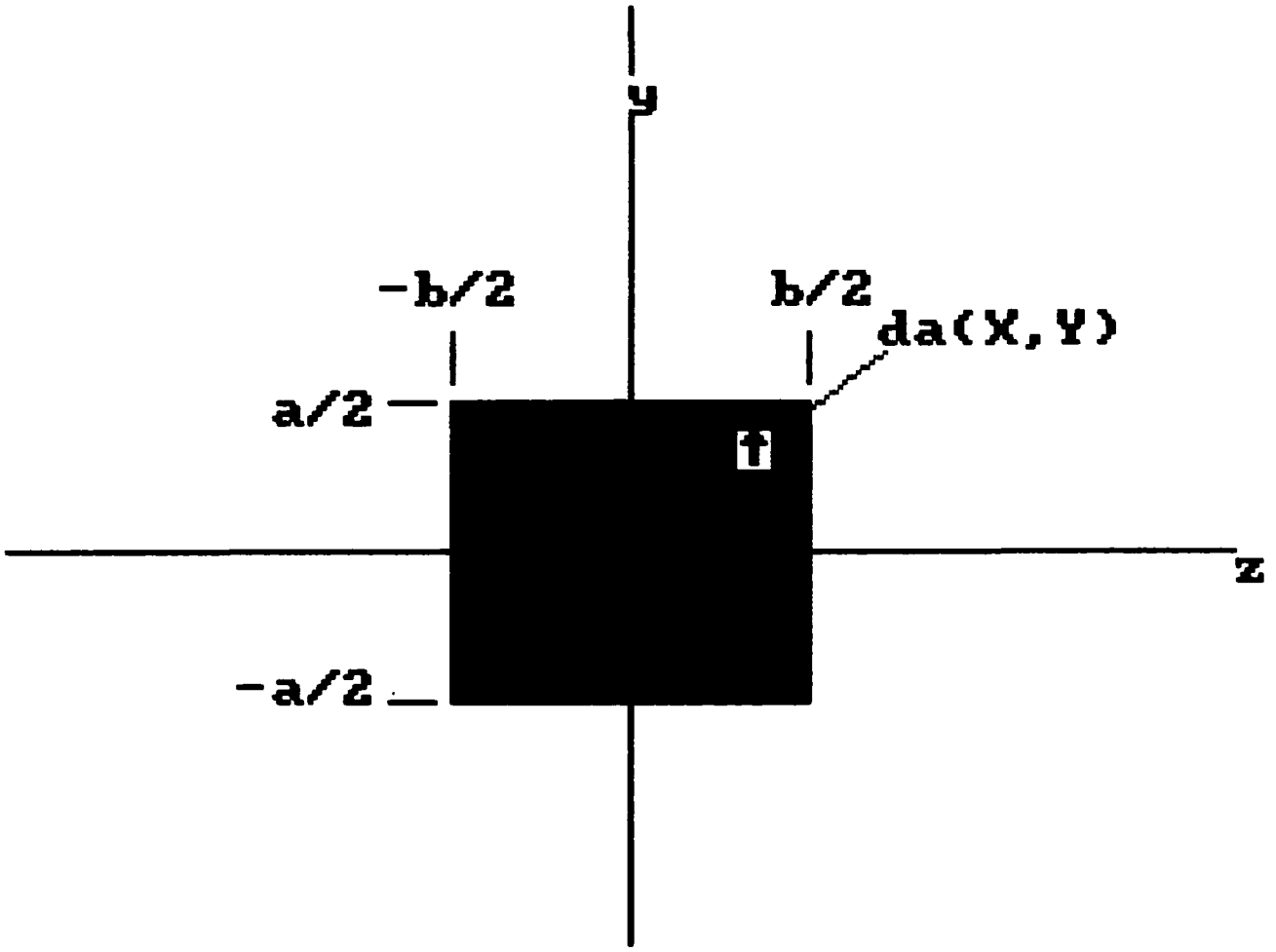

Figure 9. The coordinate system for integrating over the finite y and z dimensions.

21:43:03
21:43:25

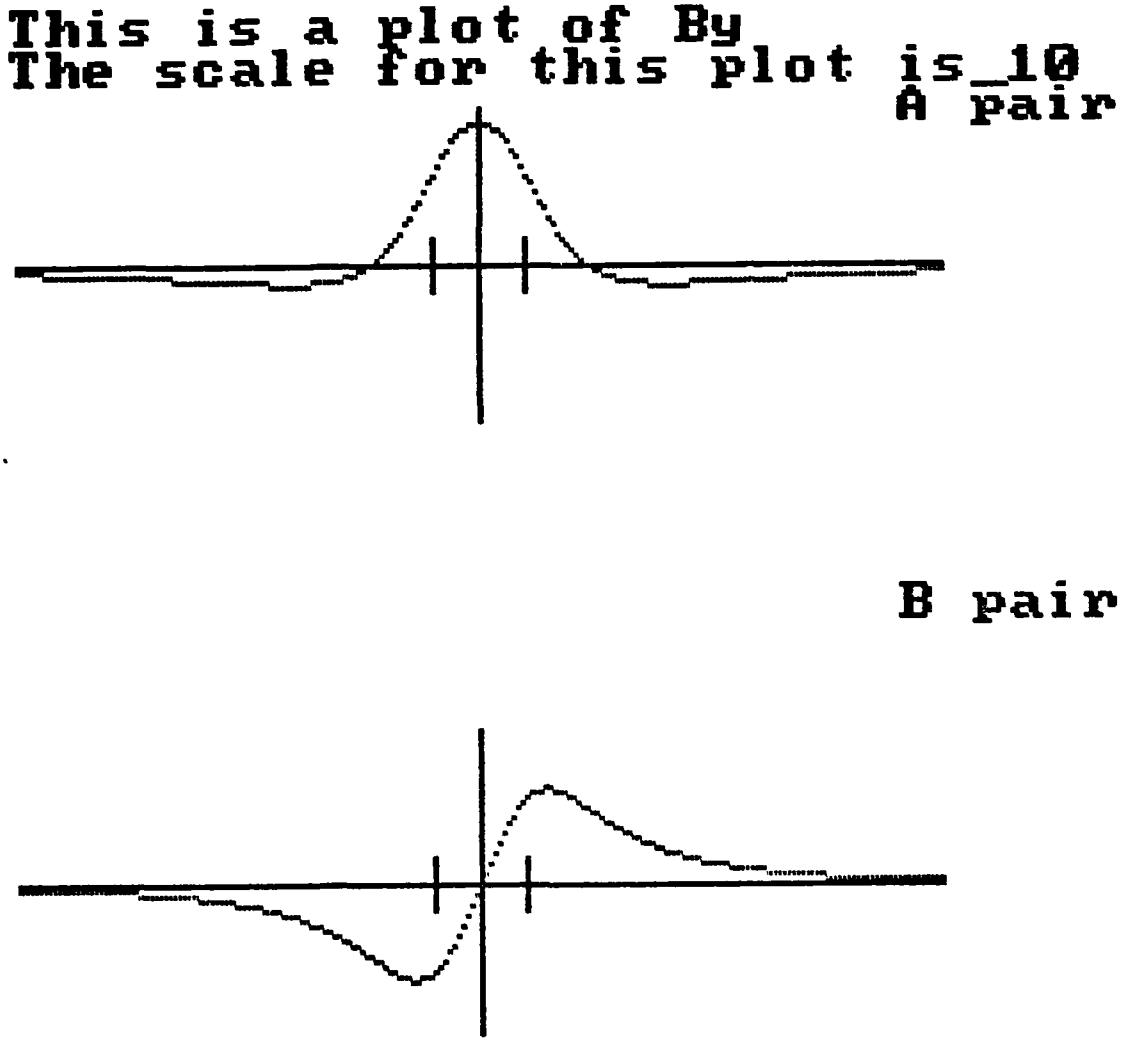

Figure 10. The y component of the magnetic field. The short vertical lines indicate the edges of the magnets.

21:45:18
21:45:40

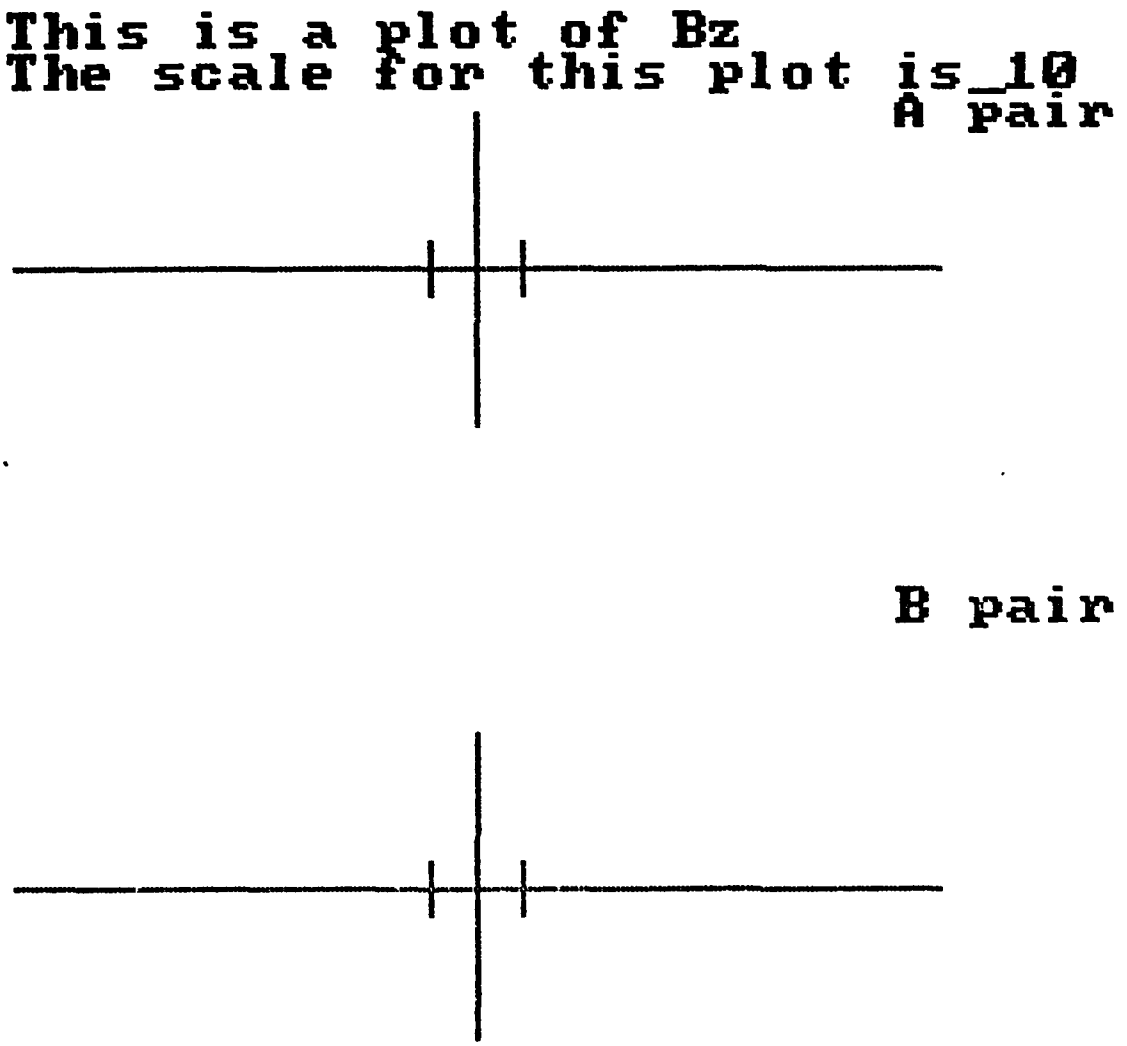

Figure 11. The z component of the magnetic field on axis is zero.

21:49:51
21:50:13

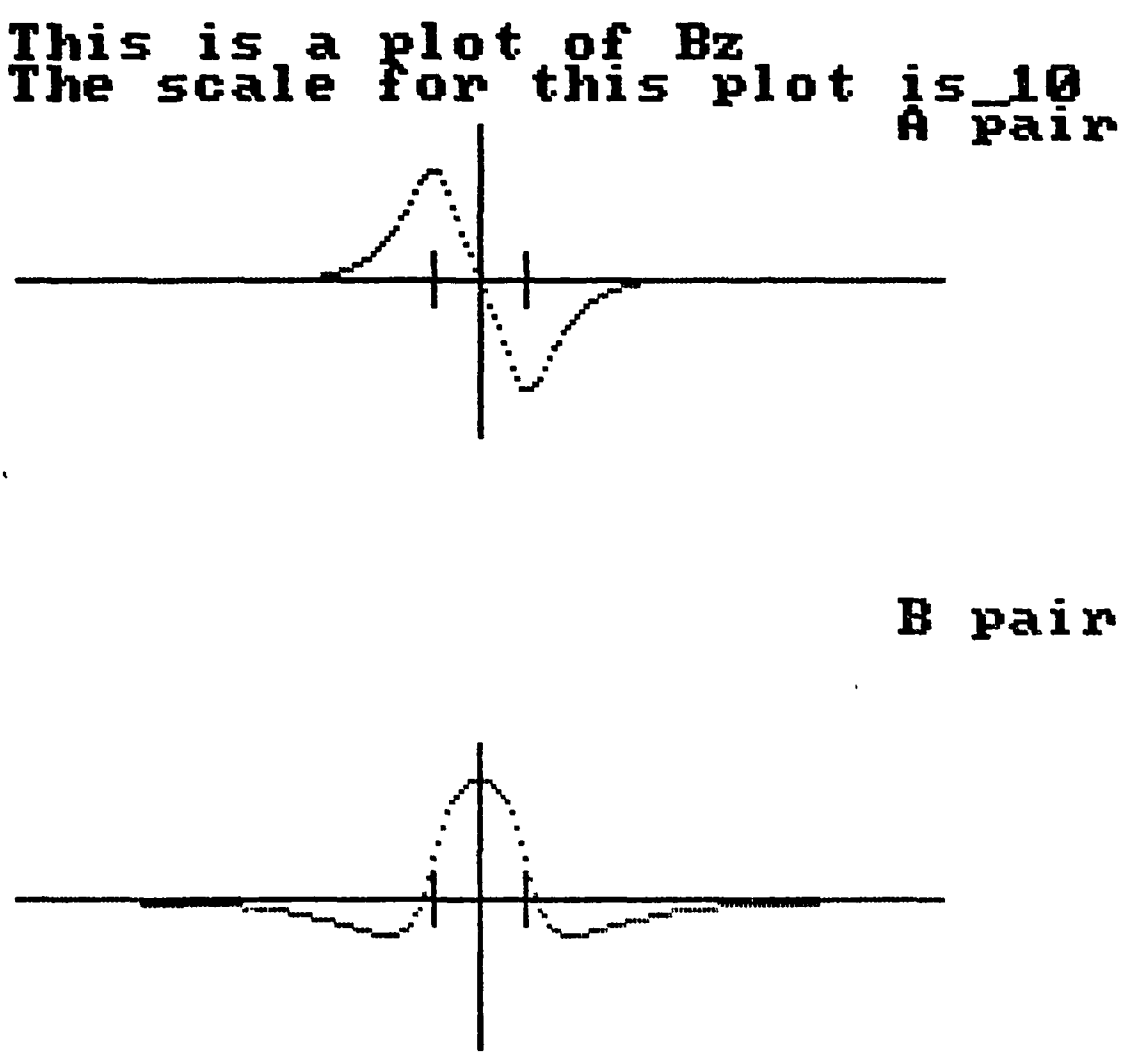

Figure 12. The z component of the magnetic at a point 5 millimeters above the axis.

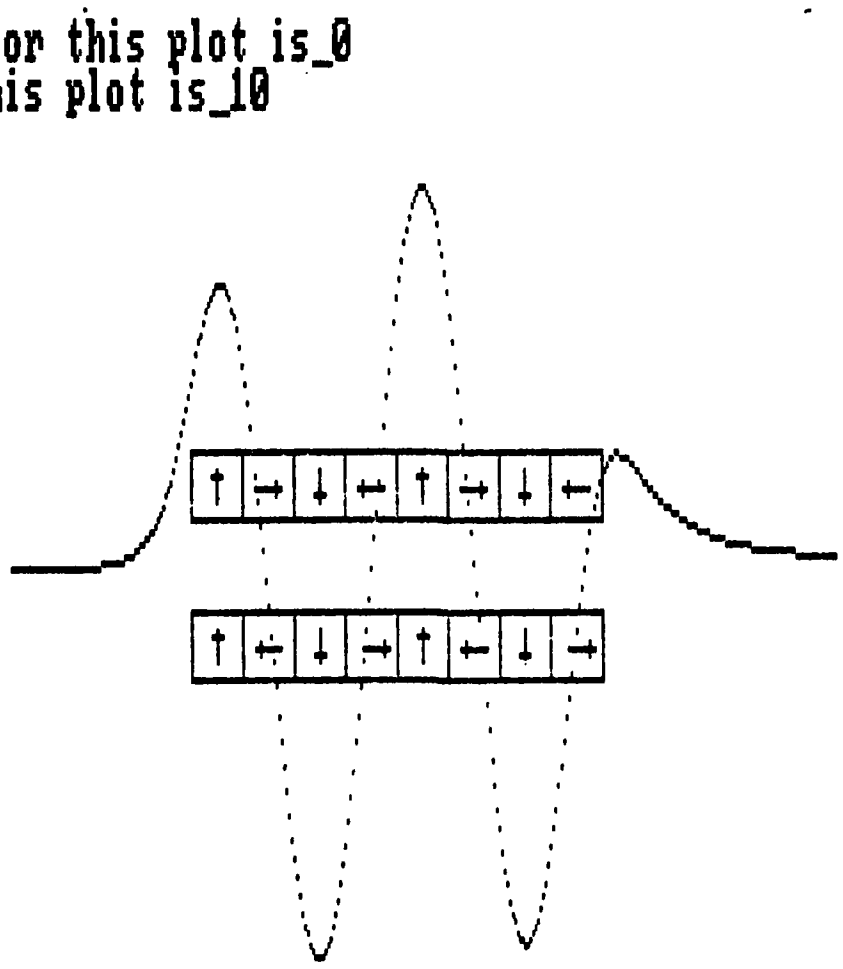

Figure 13. The y component of the magnetic field on the axis of a two period wiggler.

The value of y for this plot is_.5
The scale for this plot is_10

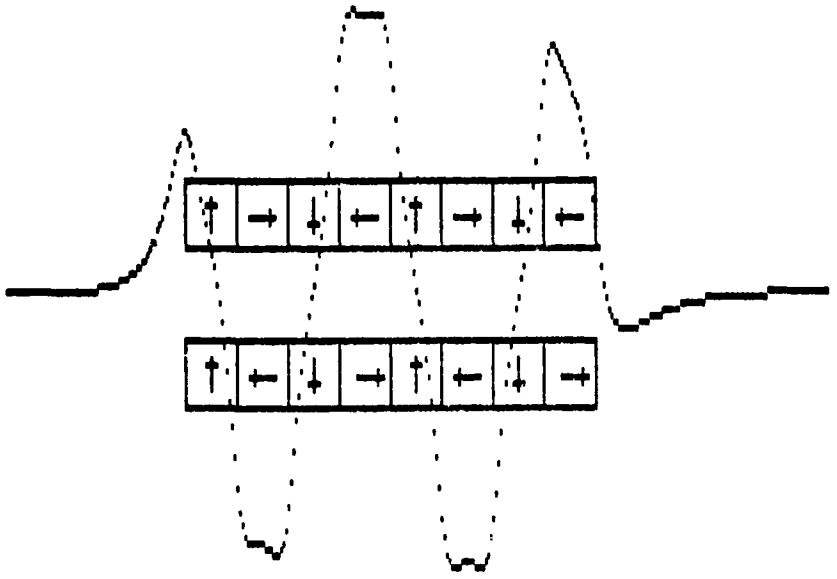

Figure 14. The z component of the magnetic field 5 millimeters above the axis of a two period wiggler.

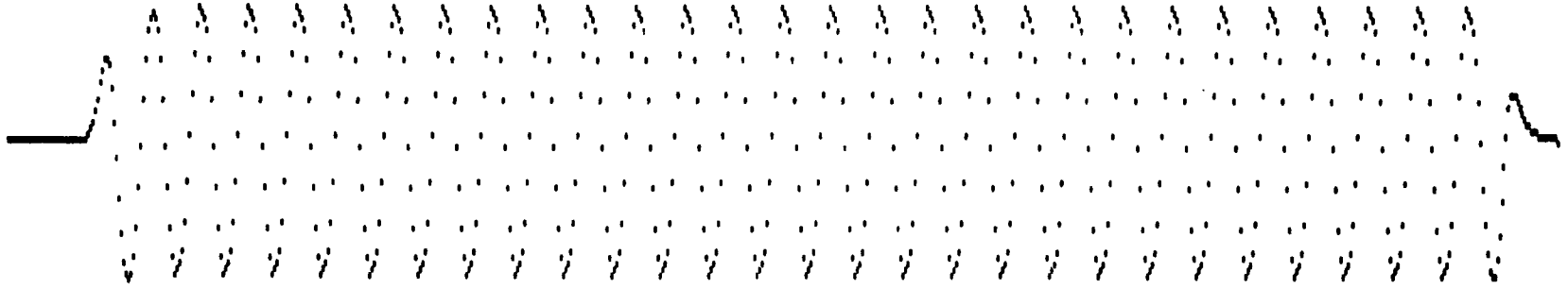

Figure 15. The y component of the magnetic field of a thirty period wiggler with a compensating magnet placed at the left hand end of the structure.

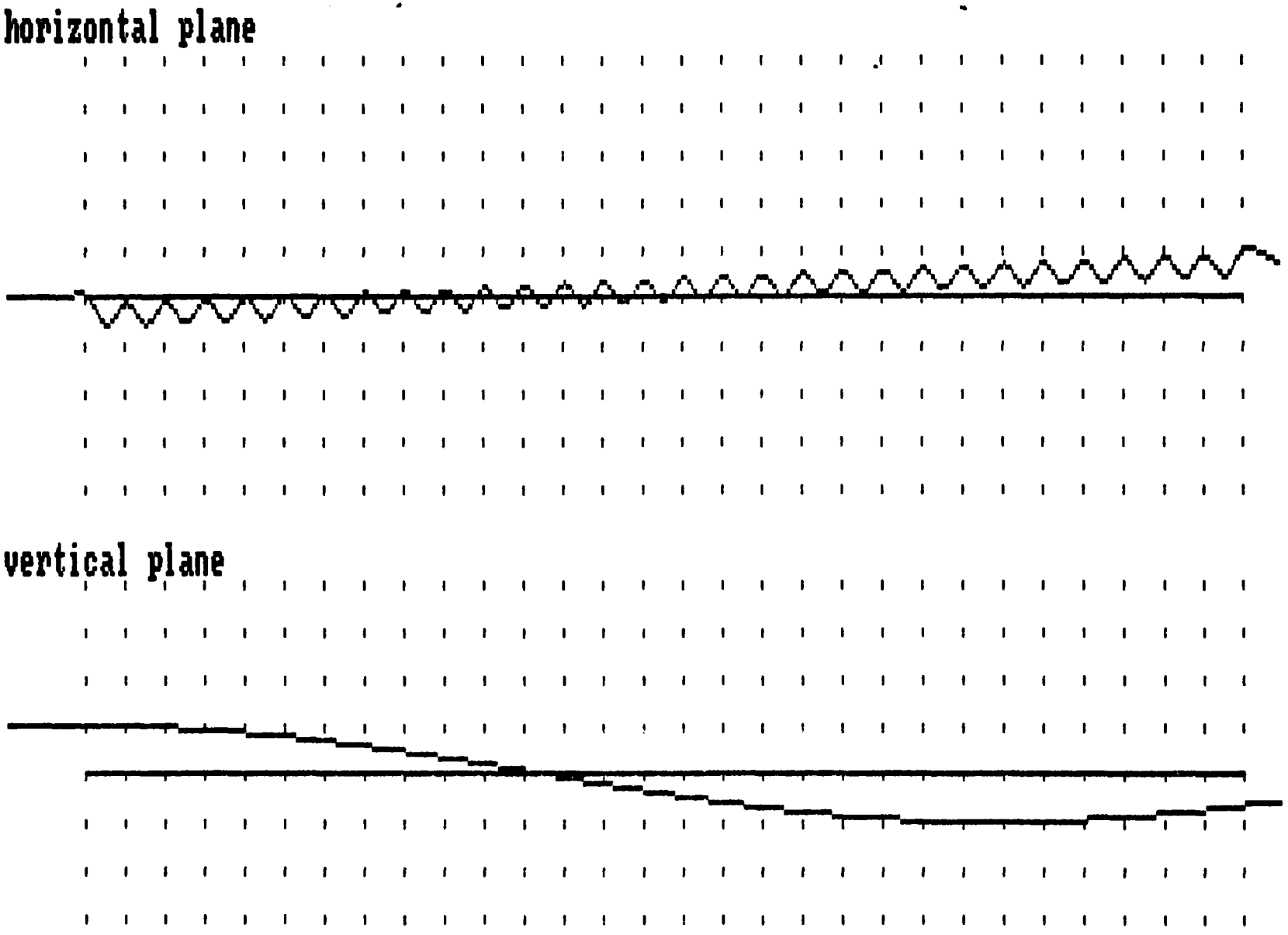

Figure 16. The output of the complete raytracing code for the parameters of the NRL FEL wiggler. The vertical tic marks are one millimeter spacings. The compensating magnets have been positioned to almost correct the path of an electron entering parallel to the wiggler axis.

END

FILMED